ELSEVIER

International Journal of Pharmaceutics 221 (2001) 123–141

international journal of pharmaceutics

www.elsevier.com/locate/ijpharm

Thermoanalytical and spectroscopic characterisation of solid-state retinoic acid

V. Berbenni *, A. Marini, G. Bruni, A. Cardini

CSGI, Dipartimento di Chimica Fisica, Università di Pavia, Viale Taramelli 16, 27100 Pavia, Italy

Received 3 January 2001; received in revised form 26 March 2001; accepted 27 March 2001

Abstract

Thermoanalytical (differential scanning calorimetry (DSC), thermogravimetric analysis (TGA), thermogravimetric analysis coupled with Fourier transform infrared spectroscopy (TG/FTIR)) and spectroscopic (X-ray diffraction (XRD), ultraviolet–visible (UV–Vis), mass spectrometry (MS) and Fourier transform infrared diffuse reflectance (DRIFT) measurements have been used to characterise solid-state retinoic acid (RA) from a chemico-physical point of view. Between 130 and 160°C, a phase transition takes place that does not correspond to the transition between the known monoclinic and triclinic phases (DSC and XRD evidence). By annealing in air (in the 130–160°C temperature range and for different times), an exothermic oxidative degradation occurs that, depending on the thermal treatment, competes with the mentioned phase transition (TGA evidence). Spectroscopic techniques (UV–Vis, MS and DRIFT) allow one to conclude that the new solid phase is still constituted by retinoic acid with a different orientation of the side chain. Finally, RA does not undergo stable melting: the fragmentation patterns, both in air and in nitrogen, have been examined by TG/FTIR.

Keywords: All-trans retinoic acid; Tretinoin; Solid-state characterisation; Phase transition

1. Introduction

Retinoic acid (3,7-dimethyl-9-(2,6,6-trimethyl-1-cyclohexen-1-yl)-2,4,6,8-nonatetraenoic acid) (RA in the following), is the vitamin A acid. Two configurational isomers exist, the 13-*cis*-retinoic acid and all-trans retinoic acid, both of them very important for their natural function (Vaezi et al., 1994; Alam et al., 1995).

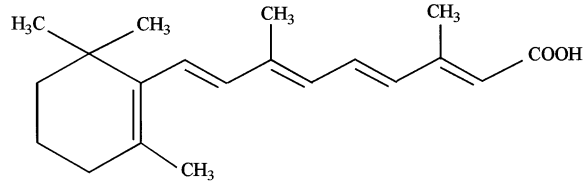

all-trans retinoic acid

Since RA plays an important role in controlling gene expression, it has found applications in the prevention and treatment of cancer, the major therapeutic successes having up to now been ob-

* Corresponding author. Tel.: +39-382-507211; Fax: +39-382-507575.

E-mail address: berbenni@fisav.unipv.it (V. Berbenni).

0378-5173/01/$ - see front matter
PII: S0378-5173(01)00677-9

tained in certain leukaemias (Muccio et al., 1996, 1998). RA is also employed in dermatology (Levin et al., 1994), namely in the treatment of skin diseases such as acne, psoriasis and skin cancer. On the other hand, the ability of some cationic polyelectrolytes to immobilize RA has spurred the engineering of new materials with interesting structural and optical properties (Thunemann, 1997; Thunemann et al., 2000).

A great deal of information exists on the pharmaceutical applications of RA, while the study of its solid-state physico-chemical properties has

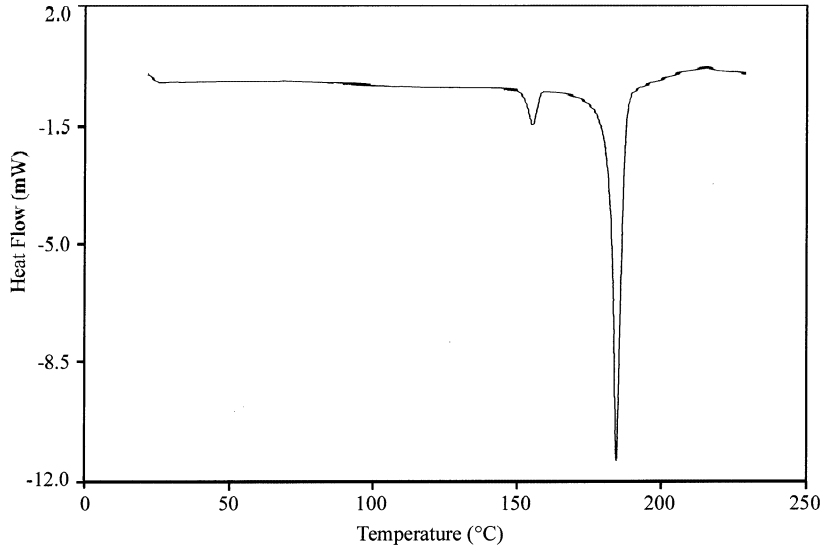

Fig. 1. A DSC thermal trace of a commercial sample of all-trans retinoic acid (nitrogen flow, 5°C/min).

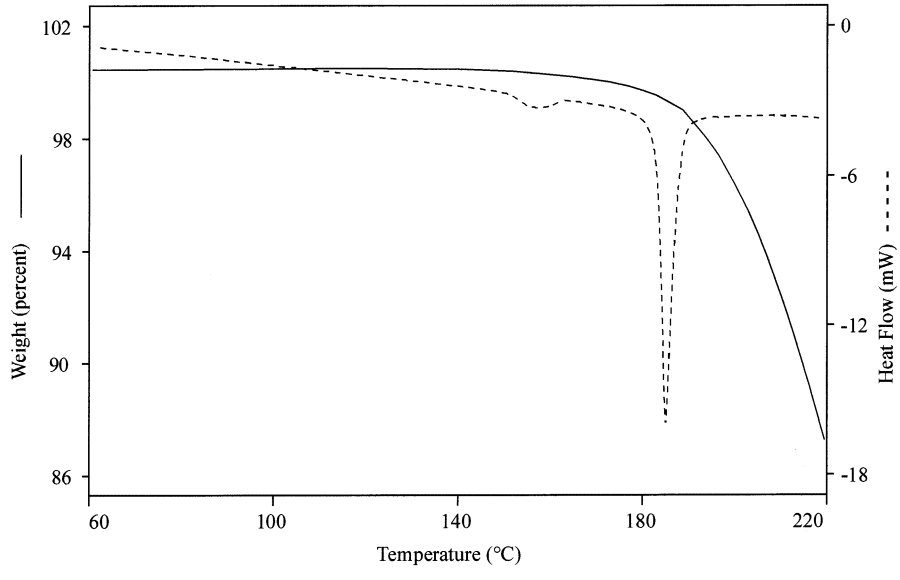

Fig. 2. Simultaneous TG/DSC trace of a commercial sample of all-trans retinoic acid (nitrogen flow, 5°C/min). Solid line, TG signal; dashed line, DSC signal.

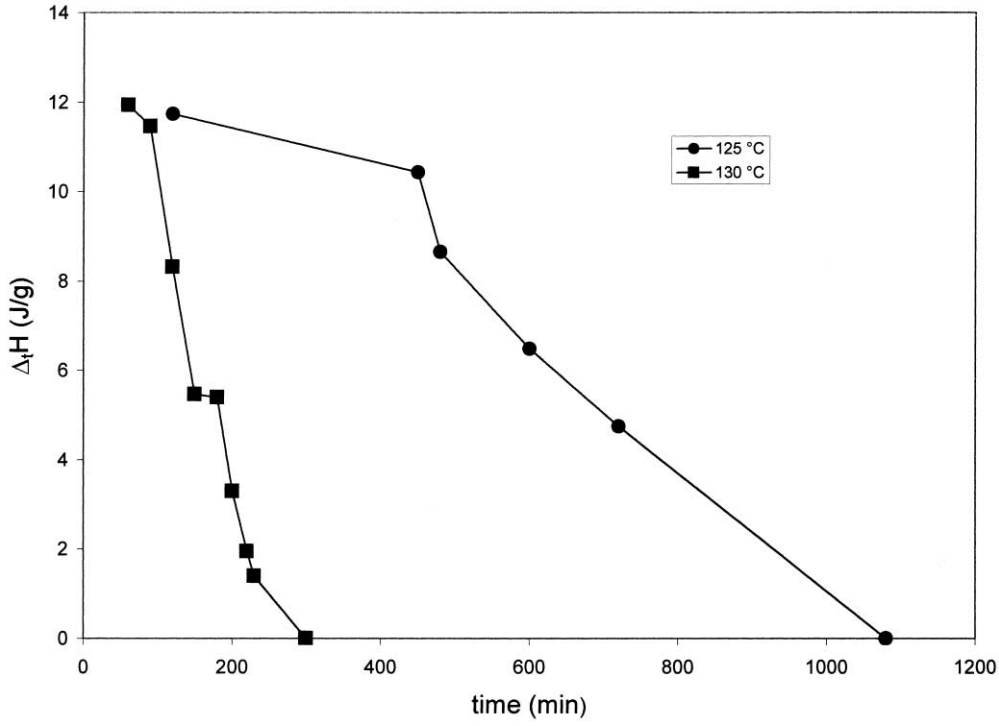

Fig. 3. Area of the endothermic DSC peak at 150°C ($\Delta_t H$, J/g) as a function of annealing time: circles, annealing at 125°C; squares, annealing at 130°C.

been only seldom undertaken. Namely, a structural study has been performed and two different crystallographic forms of RA have been brought into evidence. According to Stam and McGillavry (1963), a triclinic form of RA can be obtained by heating, at 120°C, the monoclinic form (Stam, 1972). It has to be noted that the monoclinic form would be less stable (by about 2.5 kcal/mol) and, this notwithstanding, it is the form obtained at room temperature (RT). Another paper (Tan et al., 1992) examines (by microcalorimetry and high-performance liquid chromatography) the thermal stability of all-trans RA and 13-*cis*-RA. This work reports differential scanning calorimetry (DSC) measurements showing that the 13-*cis* isomer melts at 180°C, while the all-trans RA, before melting, displays an endothermic peak at 150°C that would be due to the monoclinic–triclinic transition.

The present work will report the results obtained in a physico-chemical characterisation of solid-state all-trans RA. To this aim, use has been made of both thermoanalytical (DSC, thermogravimetric analysis (TGA) both alone and coupled with Fourier transform infrared spectroscopy (TG/FTIR) of the evolved gases) and

Table 1
TGA data of measurements performed at $T < T_{fus}$[a]

T (°C)	ΔM (%) air	ΔM (%) N_2
60	+0.40	−0.04
80	+0.22	−0.11
100	+0.24	−0.17
120	+0.70	−0.35
130	−0.60	−0.98
140	−13.54	−2.68
150	−9.81	−7.14
160	−0.93	−21.65
170	−0.43	−45.21

[a] Isothermal stages of 5 h were successively carried out at the temperatures reported. The mass loss (ΔM (%) in air and N_2) of each stage is reported.

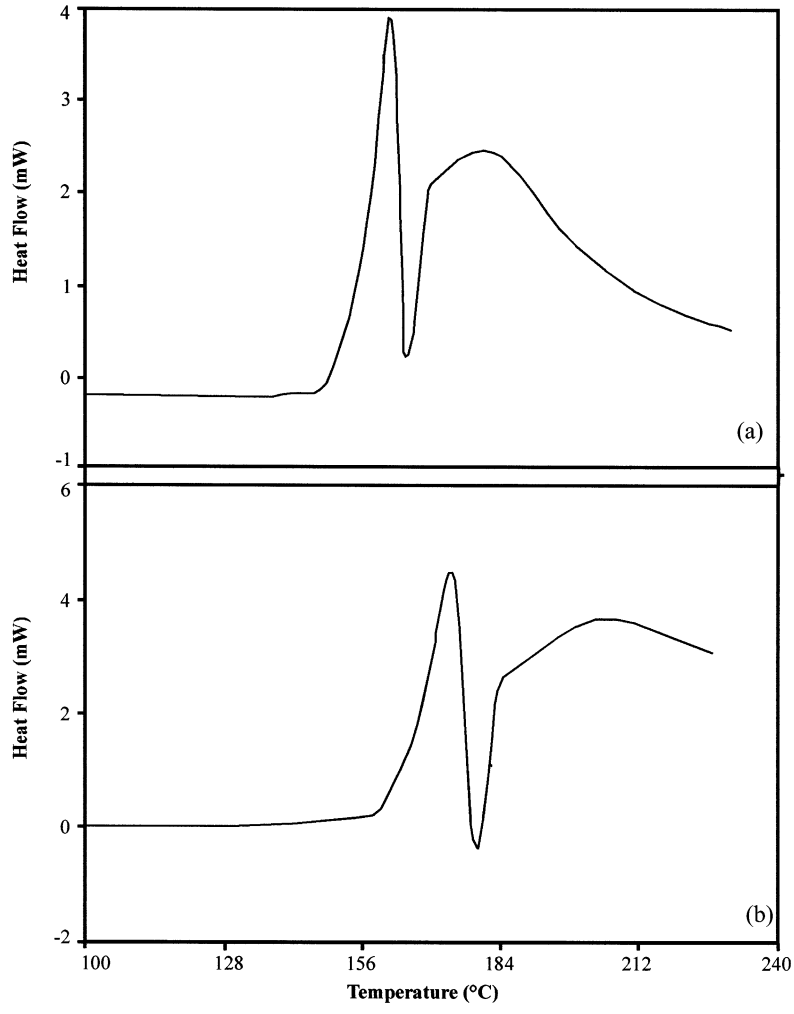

Fig. 4. DSC curves of a commercial sample of all-trans retinoic acid (air atmosphere): (a) 1°C/min, (b) 2°C/min, (c) 5°C/min, and (d) 10°C/min.

spectroscopic (FTIR diffuse reflectance, UV–Vis spectroscopy, mass spectrometry and X-ray powder diffractometry) techniques.

2. Experimental

2.1. Sample

All the measurements have been carried out on commercial all-trans RA (Sigma Aldrich, Italy). Starting from this precursor, other samples have been prepared by various thermal treatments (which will be described in due course).

2.2. Experimental techniques

Heat-flux DSC measurements were performed by a TA2920 cell connected with a TA5000 thermal analysis system (both by TA Instruments, USA). Experiments were carried out (under a dry nitrogen flux of 2 l/h) on samples of 4–5 mg that have been heated, in open or sealed Al pans, between RT and 220°C at different heating rates

(1, 2, 5 and 10°C/min). In some instances, isothermal stages of different duration (between 30 and 1080 min) and at different temperatures (in the 80–130°C range) have been inserted into the heating ramp.

Thermogravimetric measurements were performed by a DuPont 951 thermogravimetric analyser (DuPont Instruments, USA) connected with a TA3000 thermal analysis system (TA Instruments, USA). The samples (4–5 mg) were heated (under dry air or dry nitrogen flux) either dynamically (5, 10 and 20°C/min) or with isothermal stages of 5 h inserted in the ramp at different temperatures (between 60 and 170°C).

Simultaneous TGA/DSC measurements were carried out by a STA 625 TGA/DSC apparatus (Polymer Lab., UK). Samples (4–5 mg) were put in open aluminium pans and heated at 1, 2, 5 and 10°C/min up to 220°C under nitrogen flux.

The coupled TG/FTIR measurements were performed by heating RA at 5, 10 and 20°C/min (under dry air or dry nitrogen flux, 50 ml/min) between RT and 400°C. The outlet tube of the thermobalance was connected to a FTIR gas cell that was maintained at 200°C and placed inside a FTIR spectrometer (FT-IR Model 730; Nicolet,

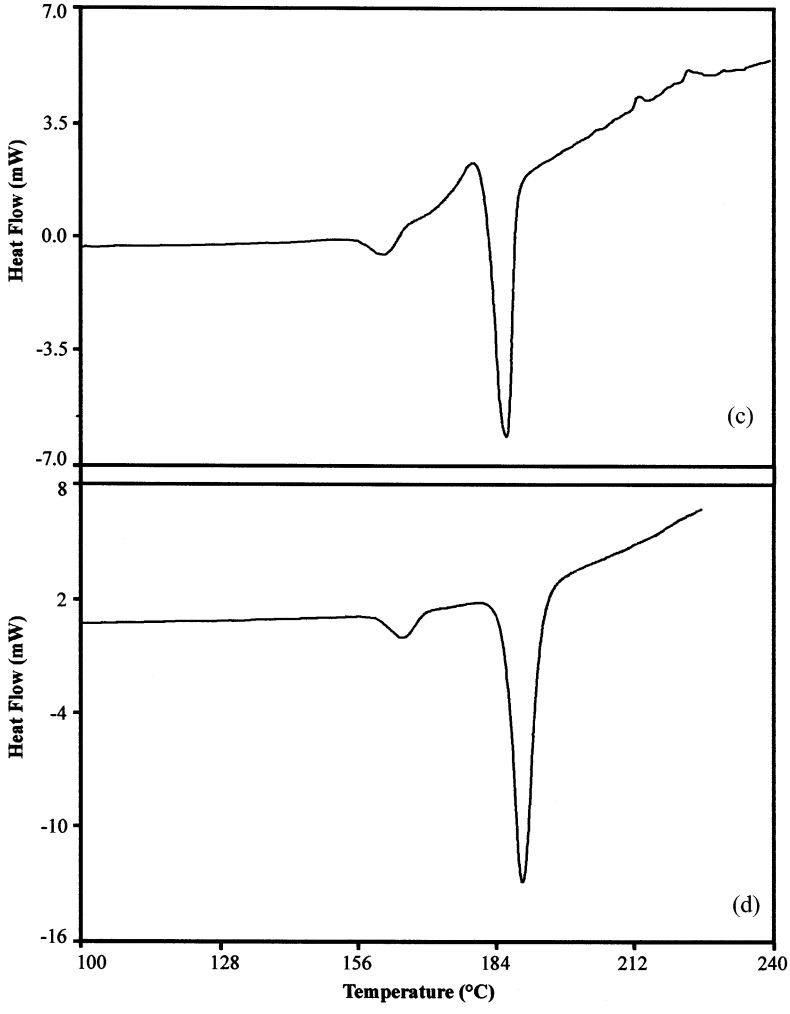

Fig. 4. (*Continued*)

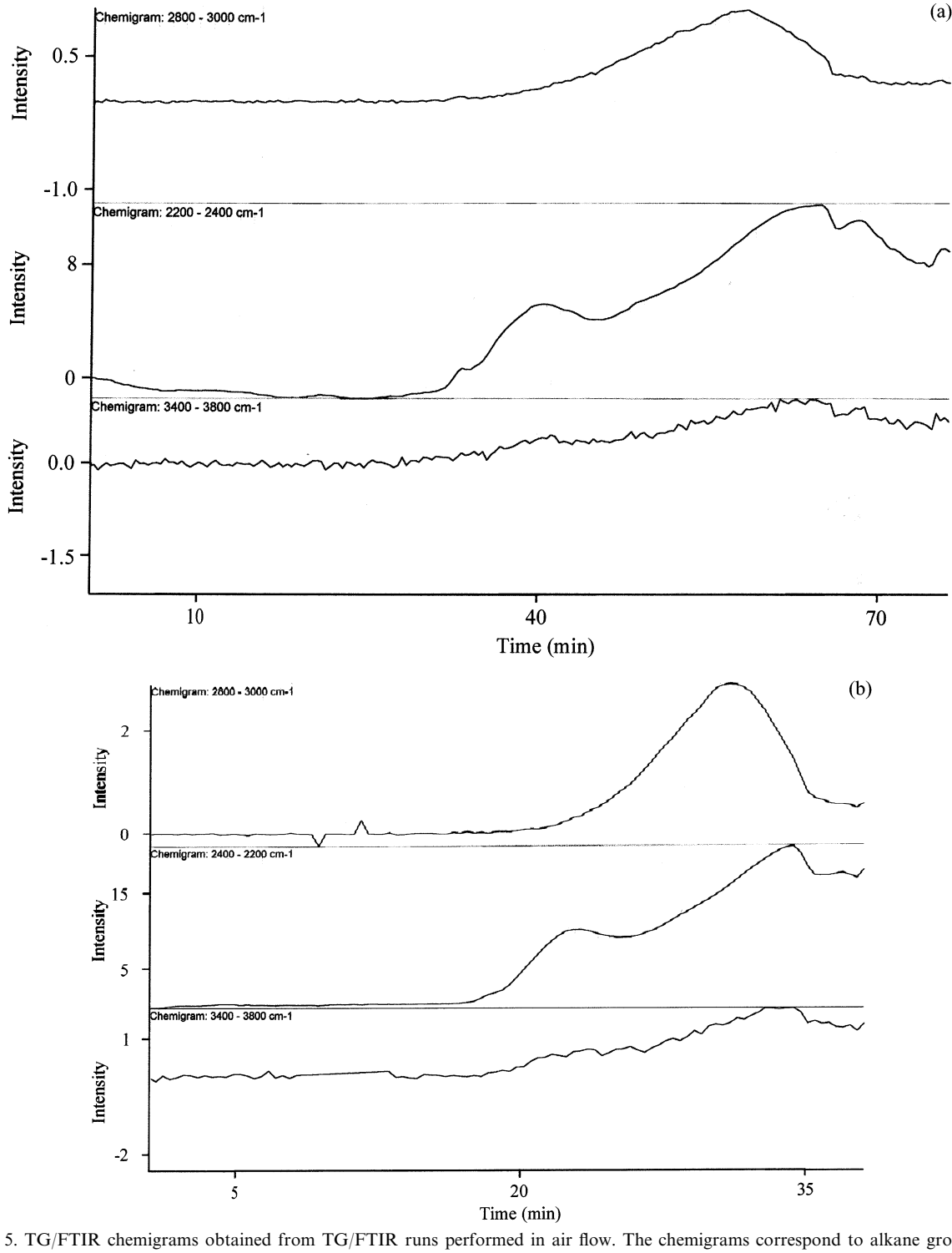

Fig. 5. TG/FTIR chemigrams obtained from TG/FTIR runs performed in air flow. The chemigrams correspond to alkane groups (2800–3000 cm^{-1}), to CO_2 (2200–2400 cm^{-1}) and to H_2O (3400–3800 cm^{-1}): (a) 5°C/min, (b) 10°C/min, and (c) 20°C/min.

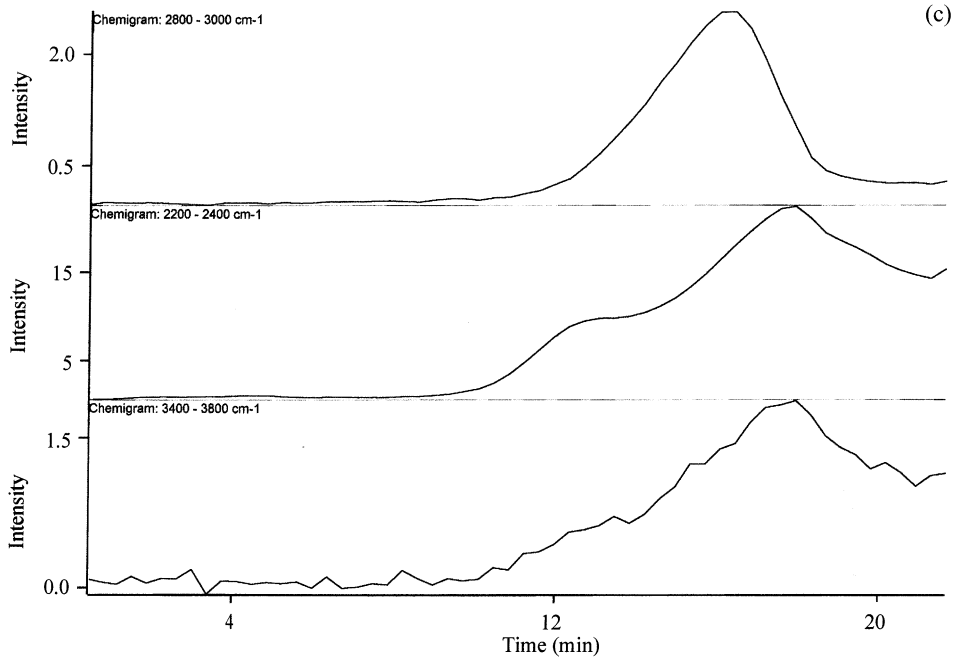

Fig. 5. (*Continued*)

USA). At the end of the run, integrated absorbance graphs (chemigrams) (Marini et al., 1994) were reconstructed as a function of time (temperature).

RA (10^{-5} M) solutions in methanol (Fluka, Switzerland) were analysed by a double-beam UV–Vis spectrometer (model V-530; Jasco Japan). The spectra have been recorded, against methanol as a blank, between 700 and 190 nm with a scanning speed of 40 nm/min and a fixed bandwidth of 2.0 nm.

A LCQ DECA mass spectrometer (FINNIGAN MAT, USA) equipped with an electron spray ionisation (ESI) source was used. The analyser consists of an ionic trap and the detector is an electronic multiplier. RA (10^{-4} M) solutions in methanol were directly injected (5 μl/min) into the ESI ionisation chamber. Spectra of both positive and negative ions were obtained by respectively setting the following experimental parameters: positive ions (source voltage, + 5 kV; capillary temperature, 100°C); negative ions (source voltage, − 5 kV; capillary temperature, 100°C).

Diffuse reflectance FTIR spectra were recorded with a FT-IR Model 730 Nicolet Spectrometer (Nicolet, USA) equipped with a diffuse reflectance attachment (Drift Collector, Spectra Tech, UK) and flushed with a dry nitrogen stream of 20 l/min. The spectra (4000–400 cm^{-1}) were collected on solid RA samples dispersed (1–2% by mass) in a KBr matrix by 2-min milling in an agate mortar. One thousand two hundred scans were co-added at 4 cm^{-1} resolution. The single-beam spectra have been ratioed against a KBr background to obtain the spectra in Kubelka–Munk units.

X-Ray powder diffraction spectra were collected by a D5005 apparatus (Bruker Siemens, Germany) equipped with a goniometer and a graphite bent crystal monochromator (Cu Kα radiation). The 2θ angular range between 4 and 30° was scanned in the step scan mode (step width, 0.02°; counting time, 2 s; 40 kV, 40 mA).

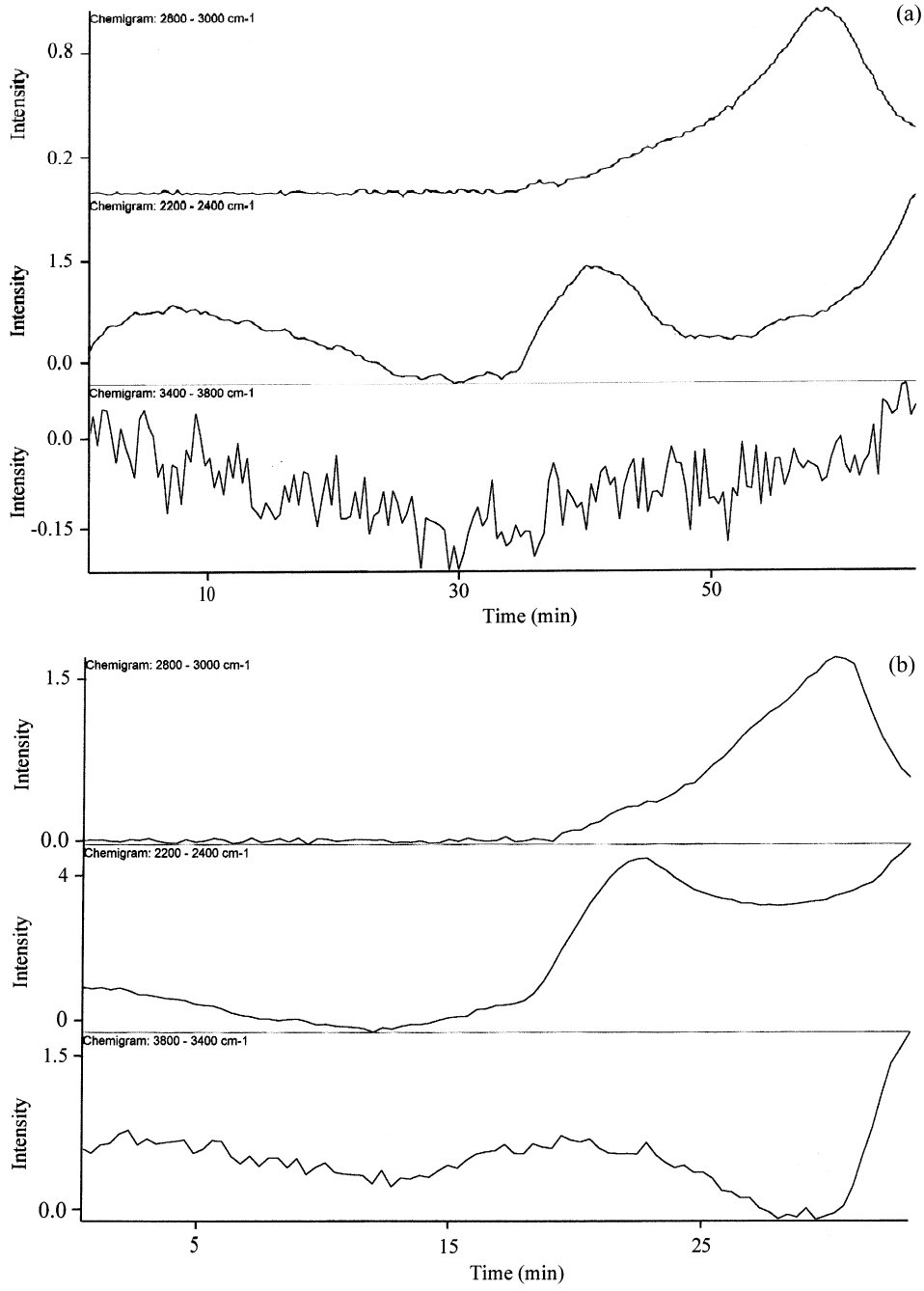

Fig. 6. TG/FTIR chemigrams obtained from TG/FTIR runs performed in nitrogen flow. The chemigrams correspond to alkane groups (2800–3000 cm^{-1}), to CO_2 (2200–2400 cm^{-1}) and to H_2O (3400–3800 cm^{-1}): (a) 5°C/min, (b) 10°C/min, and (c) 20°C/min.

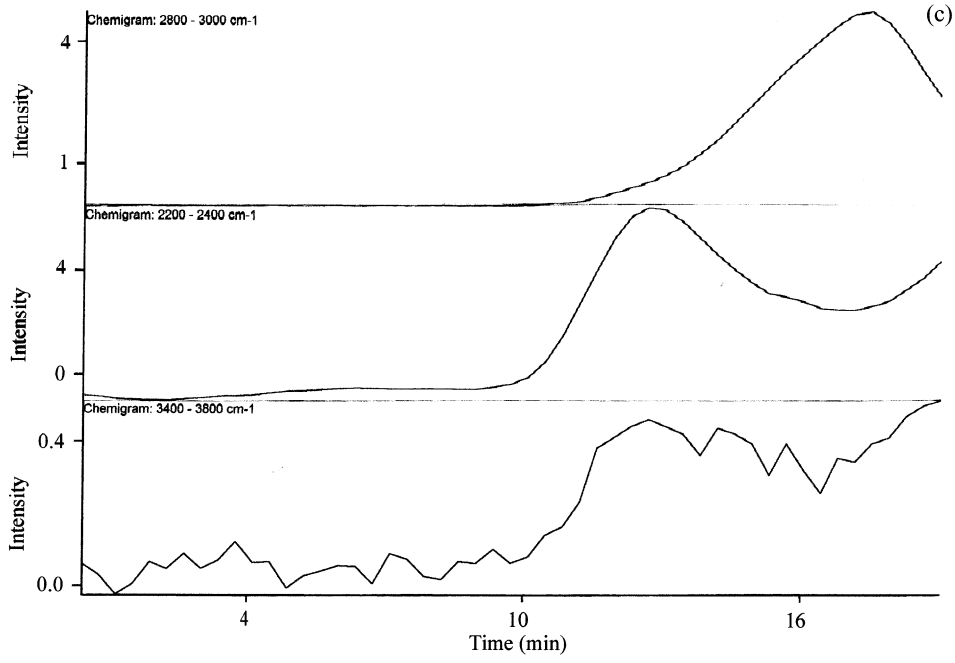

Fig. 6. (*Continued*)

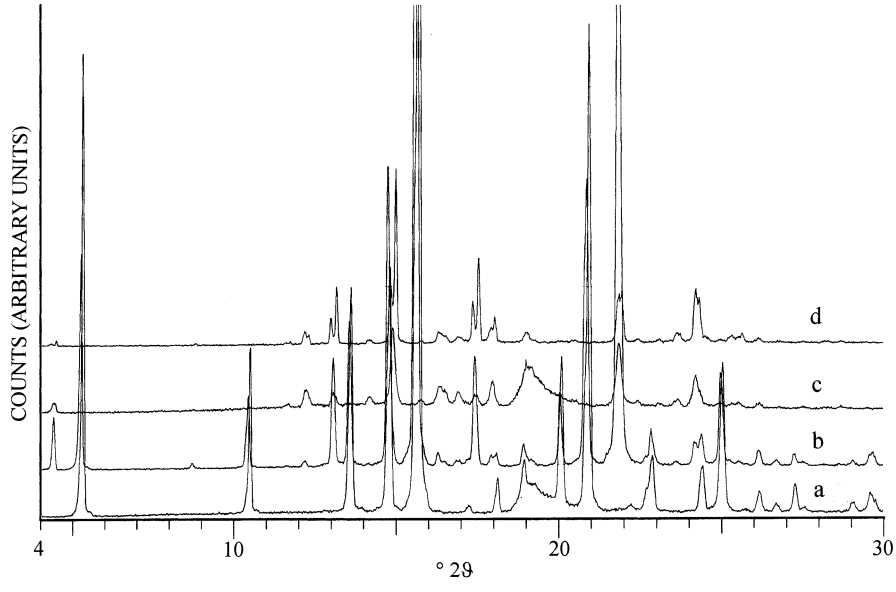

Fig. 7. XRD powder patterns of (a) a commercial sample of all-trans retinoic acid, (b) sample (a) thermally treated for 3 h at 130°C in nitrogen, (c) sample (a) thermally treated for 3 h at 130°C in air, and (d) sample (a) thermally treated for 66 h at 130°C in nitrogen.

3. Results and discussion

3.1. Thermoanalytical measurements

3.1.1. DSC measurements

Fig. 1 reports a typical DSC trace of a RA sample. Two peaks are showing: the peak at 183°C is due to the melting process while that at ~150°C will be tentatively ascribed, according to Tan et al. (1992), to the monoclinic–triclinic phase transition.

Fig. 2 reports a simultaneous TGA/DSC trace. The DSC part shows the same two peaks of Fig. 1 while the TGA signal indicates that a mass loss process takes place under the melting peak. This means that RA is not stable over melting. This point is confirmed by the fact that no DSC peaks are observed in a second heating run. The mean enthalpy values derived from the DSC peaks (from about 20 runs performed at the different heating rates) are, respectively, $\Delta_t H = 11.28 \pm 0.45$ (transition) and $\Delta_{fus} H = 130.69 \pm 5.88$ J/g (melting). If, however, the runs performed with sealed and open pans are considered separately, the mean melting enthalpies are 134.89 ± 3.75 (sealed pans) and 123.91 ± 3.07 J/g (open pans). The last value is very close to the mean enthalpy value (122.97 ± 5.78 J/g) obtained from the measurements performed in the simultaneous TGA/DSC apparatus where, obviously, open pans have been used. The fact that higher mean $\Delta_{fus} H$ values are obtained by running the samples in sealed containers can be due to some other endothermic phenomenon that occurs besides melting. Such a phenomenon is by no means a combustion process (which would be an exothermic one) or evaporation/sublimation, which cannot occur in a closed system. Therefore, we can hypothesise that there should be an endothermic thermolysis phenomenon that occurs during melting in a closed system.

Another process is also occurring over melting in an open system, as is indicated by the mass loss recorded under the melting peak. The experimental observation that such a mass loss decreases by increasing the heating rate suggests that an activated phenomenon, such as a decomposition reaction, rather than a sublimation/evaporation

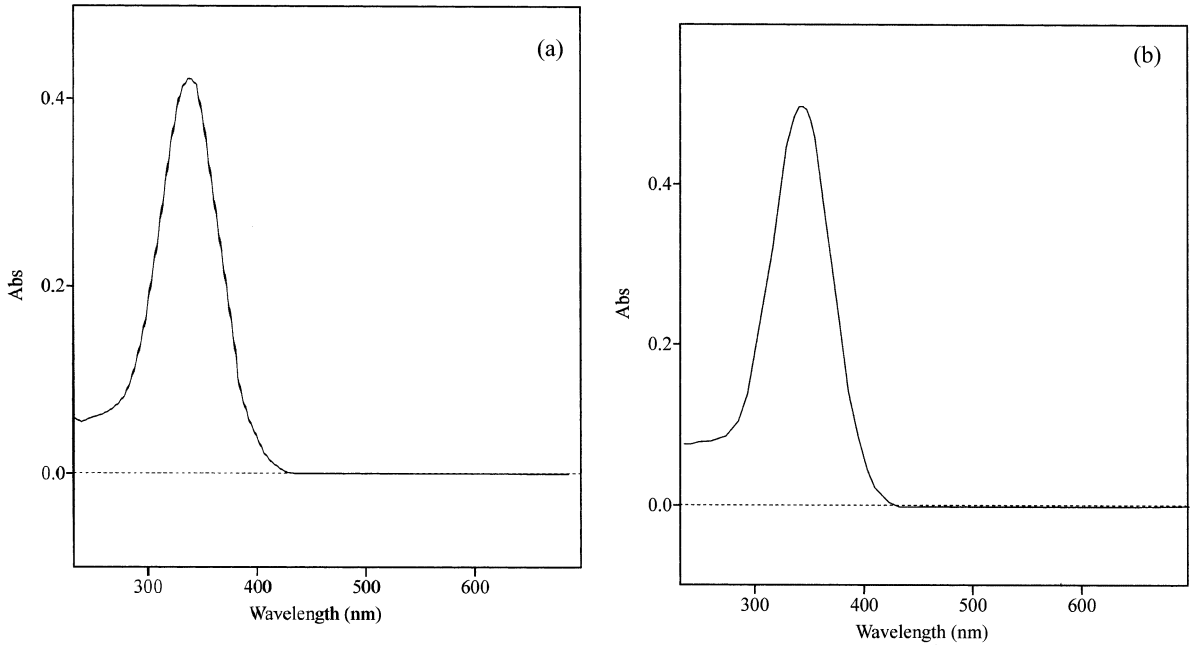

Fig. 8. UV–Vis spectra of methanolic solutions of (a) commercial all-trans retinoic acid and (b) sample (a) thermally treated for 66 h at 130°C in N_2.

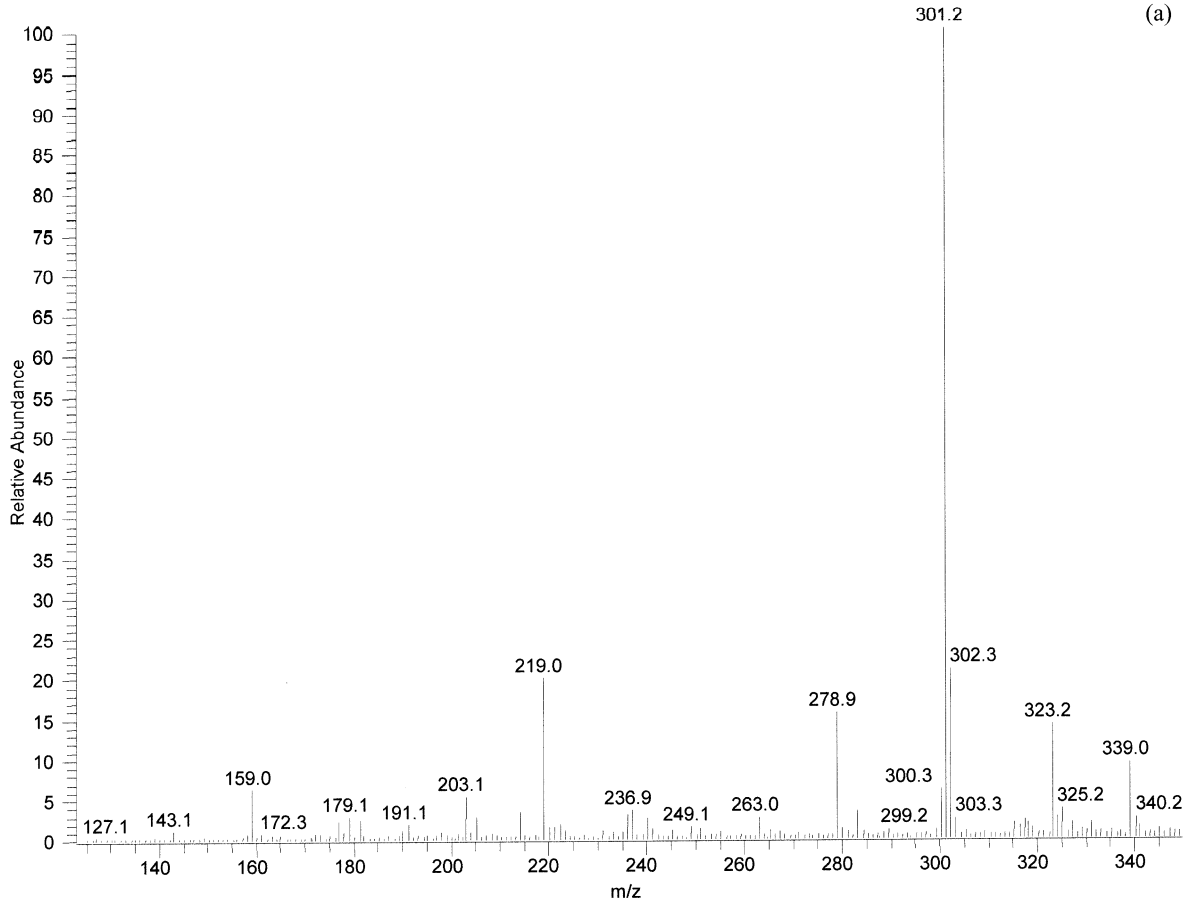

Fig. 9. Mass spectra of methanolic solutions of a commercial sample of all-trans retinoic acid: (a) positive ions, and (b) negative ions.

process is going on as RA melts. More insight into its nature will be gained by the analysis of the gaseous products released in the process (see Section 3.1.2.2).

The enthalpy of the endothermic peak at 150°C does not show any dependence on the pan type. Furthermore, it has to be noted that such a peak is only present during the first heating run. To understand the nature of the phenomenon occurring under the peak, DSC measurements have been performed with an isothermal stage inserted in the heating ramp. Namely, it has been verified that, by subjecting RA to 5 h isothermal stages at temperatures up to 120°C, no appreciable differences are obtained in both transition and melting enthalpies with respect to the dynamic runs. On the contrary, after an isothermal stage of 5 h at 130°C, the peak at 150°C disappears with the area of the melting peak being unaffected. Therefore, other DSC measurements have been performed where the samples have been annealed at 125 or at 130°C for different times. Fig. 3 shows the decreasing trend of the peak area as a function of isothermal time. It has to be noted that the decreasing trend does not depend on the sample pan (open or sealed). Therefore, as concerns the phenomenon that is at the origin of the peak at 150°C, the following considerations can be proposed.

- The isothermal experiments show that it can occur at a temperature (125–130°C) well below that of the dynamic peak (150°C) provided

enough time is elapsed at that temperature. Therefore, a kinetic factor is playing an important role in the transformation. The thermodynamic temperature of the phenomenon should be at a lower temperature, probably between 120 and 125°C. It is likely that the endothermic peak at 150°C that is present in the dynamic DSC scans represents the faster part of a transformation that begins at $\sim$130°C and ends at $\sim$160°C.

- From the isothermal experiments performed at 125 and 130°C, it can be seen that the peak disappears after about 1000 min (at 125°C) and 230 min (at 130°C). Thus, the phenomenon under the peak is strongly activated. This again confirms that a kinetic factor is operative in the transformation.
- In all cases, the area of the melting peak does not appear to be appreciably affected by the isothermal annealing at 125–130°C.

3.1.2. TGA and TG/FTIR

The thermal measurements performed so far have shown that, after a solid-state transformation, RA undergoes decomposition over melting. To gain some more information on the solid-state processes occurring in RA, TGA measurements have been performed below melting point. Furthermore, to analyse the mechanism of degradation during melting, TGA measurements have also been performed above melting point. In these measurements, thermogravimetry has been coupled with FTIR analysis of the evolved gases.

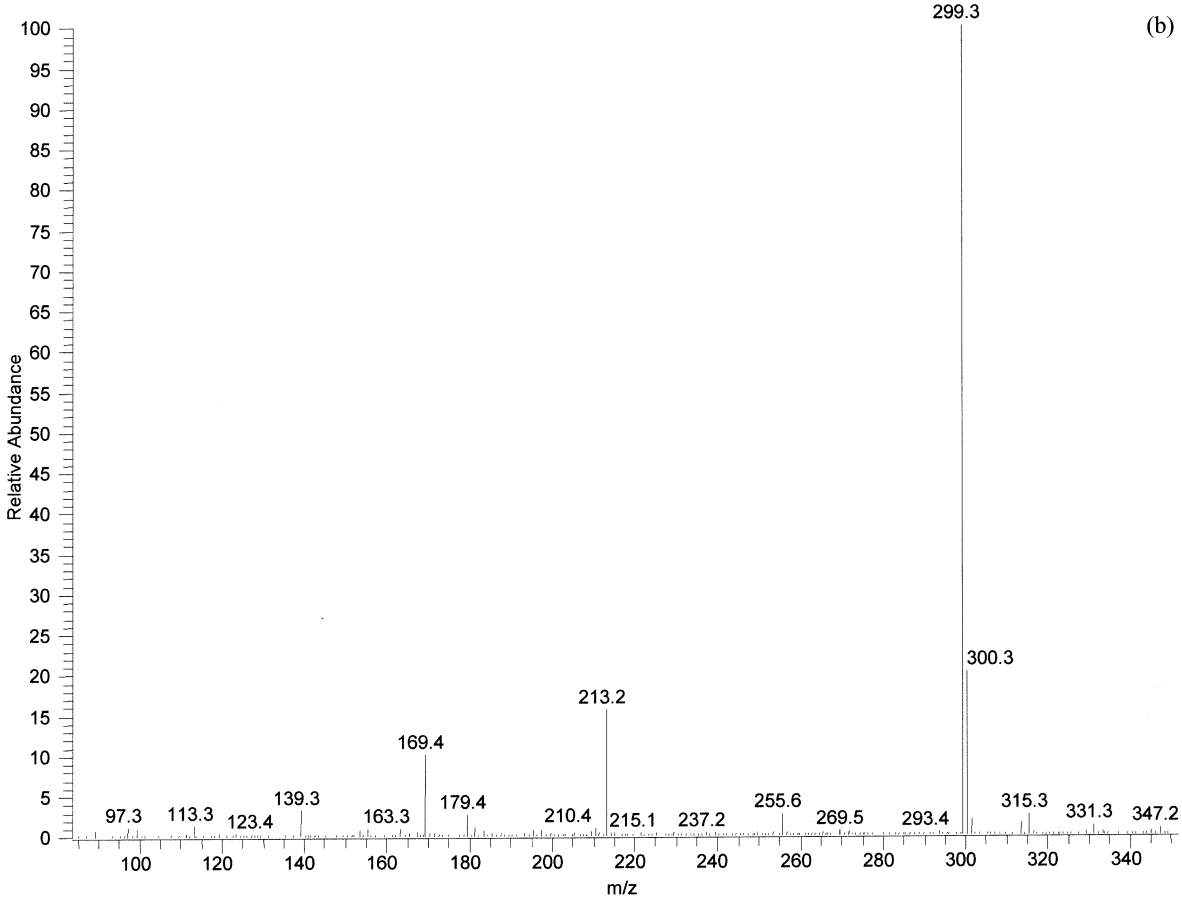

Fig. 9. (*Continued*)

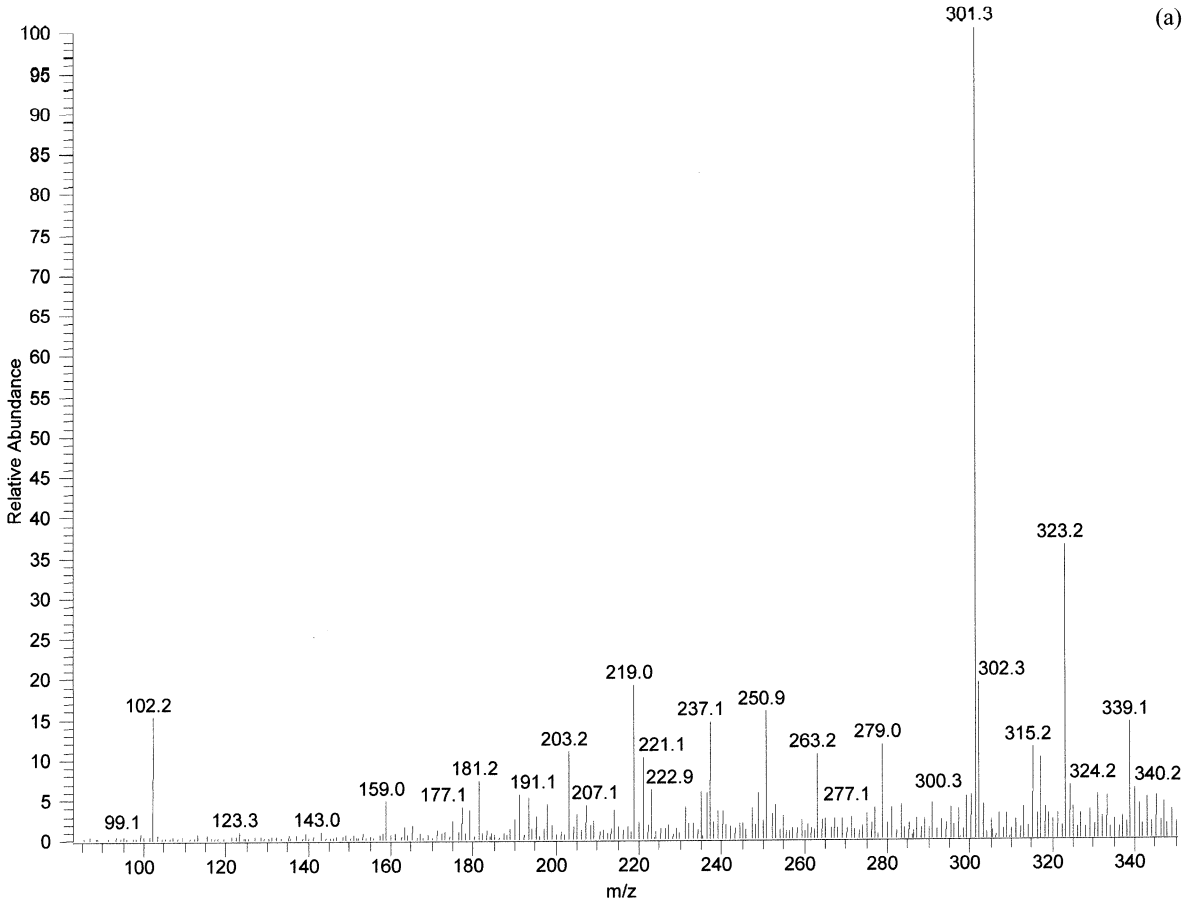

Fig. 10. Mass spectra of methanolic solutions of a thermally treated (66 h at 130°C in nitrogen) sample of all-trans retinoic acid: (a) positive ions, and (b) negative ions.

3.1.2.1. TGA measurements below the melting point. The measurements have been performed by heating the sample (both under air and nitrogen flow) up to increasing temperatures (60, 80, 100, 120, 140, 150, 160 and 170°C) where the sample has been annealed for 5 h. Table 1 reports the mass changes recorded during each of the isothermal steps. From the table, it can be seen that the thermal stability up to 140°C strongly depends on the atmosphere. Indeed, the mass loss after the isothermal stage at 140°C is -4.3% under nitrogen while under air it is -14.5%, which happens to nearly coincide with the mass loss expected for RA decarboxylation (-14.65%). Maybe this is only a coincidence. Another hypothesis stems from the mass gain ($+1.56\%$) up to 120°C that, in air, could be the result of oxygen intake; consequently, the mass loss up to 150°C could come from an oxidative degradation of RA to give fairly thermal stable product(s) (see the particularly low mass losses at 160 and 170°C). To evaluate the likelihood of such a hypothesis, DSC scans have been carried out, under air flow and with open pans, at different heating rates (1, 2, 5 and 10°C/min). The thermograms (Fig. 4a–d) show that an exothermic peak instead of the transition peak precedes the melting endotherm at the lower heating rates (1 and 2°C/min). At the higher heating rates (5 and 10°C/min), the thermograms more (10°C/min) or less (5°C/min) resemble those typically recorded in nitrogen (see Fig. 1). Therefore, provided a slow enough heat-

ing rate is used, an exothermic phenomenon takes place in air before melting, instead of an endothermic one. The exothermic peak suggests that in air an oxidative degradation takes place before melting instead of solid-state transformation, provided enough time is elapsed.

On the contrary the mass loss in N_2 becomes significant at $T > 130$°C, i.e. when, as shown by the DSC isothermal experiments, the solid-state transformation should be underway. Furthermore, it has to be said that, at the end of the run under N_2, residues of sublimated RA (not found after the run under air) were found on the cold parts of the thermobalance. This suggests that, under nitrogen, the mass loss begins after solid-state transformation and is due to RA sublimation.

3.1.2.2. TG/FTIR measurements. TGA measurements have also been performed dynamically (both under air and N_2 flow) at 5, 10 and 20°C/min to evaluate the decomposition patterns over melting. From these measurements, the chemigrams have been reconstructed (Fig. 5a–c and Fig. 6a–c report the chemigrams obtained by the TGA runs performed at different heating rates, respectively, under air and nitrogen flow). The chemigrams 2200–2400 and 3400–3800 cm^{-1} indicate, respectively, the presence of CO_2 and H_2O in the gas streams released from the sample. The chemigram 2800–3000 cm^{-1} is due to molecular fragments containing hydrocarbon groups.

The chemigrams of the TG/FTIR runs performed under air (Fig. 5a–5c) bring into evidence the following points.

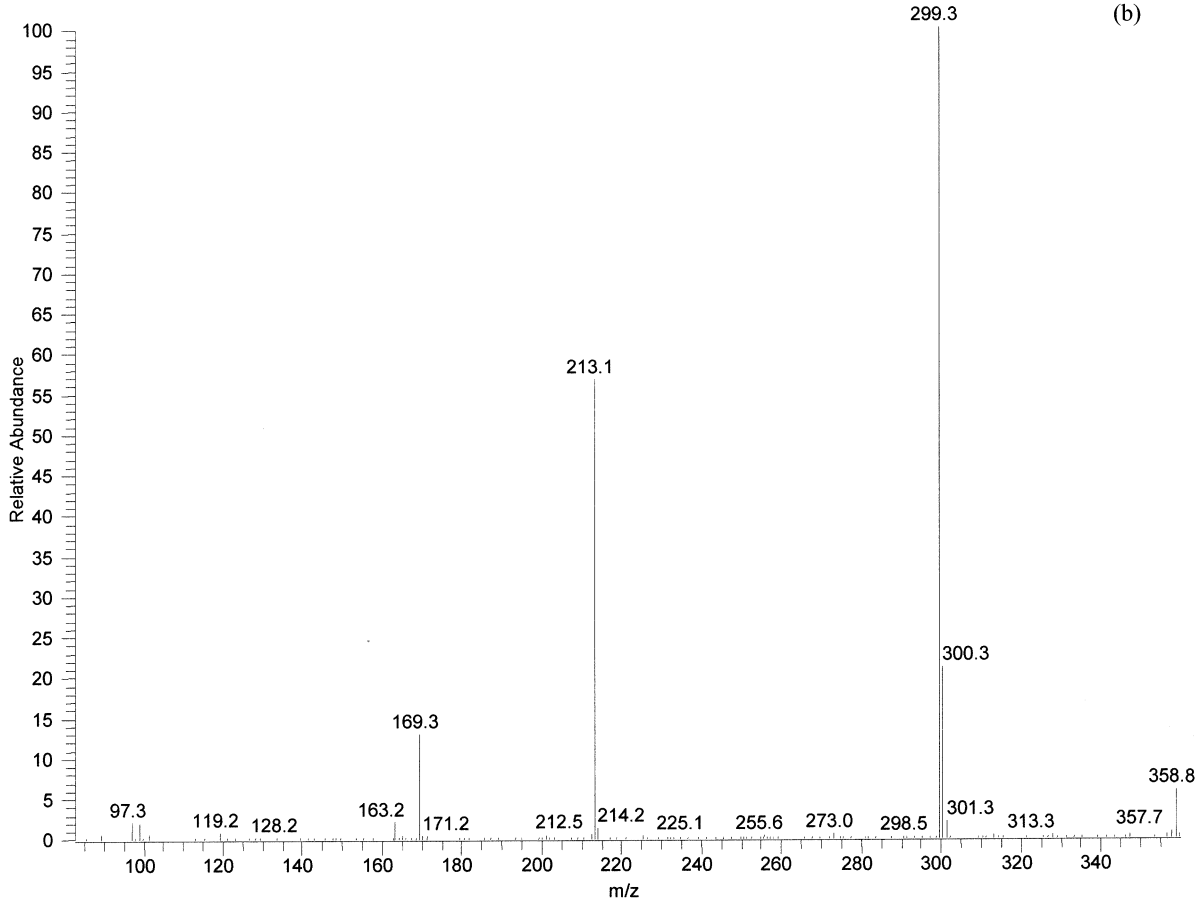

Fig. 10. (*Continued*)

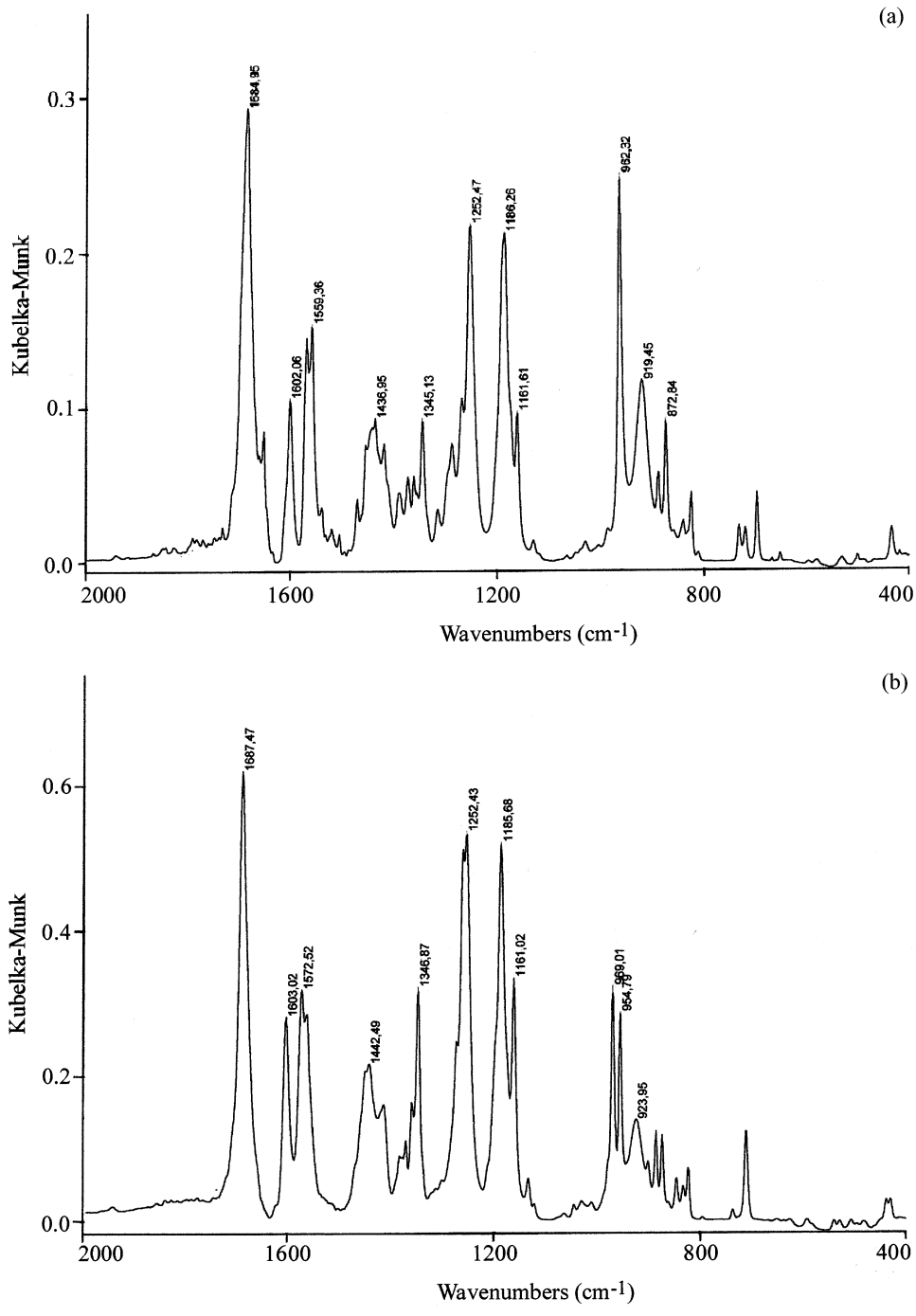

Fig. 11. Diffuse reflectance IR spectra of (a) a commercial sample of all-trans retinoic acid, and (b) sample (a) thermally treated (66 h at 130°C in nitrogen).

- The gas evolution begins to be signalled at temperatures that are, at all heating rates, higher than the melting point.
- The CO_2 evolution takes place in two subsequent stages. Since no appreciable water evolution occurs during the first peak (at least at 5 and 10°C/min; see Fig. 5a,b), it is likely that the first stage of CO_2 release corresponds to RA decarboxylation.
- Between the two CO_2 evolution peaks, the peak of the hydrocarbon groups is reached. This reveals that evaporation and/or further fragmentation of the decarboxylated residue is taking place. It has, however, to be noted that the intensities of the other two chemigrams (CO_2 and H_2O) are increasing. This fact suggests that, besides the evaporation of the decarboxylated residue, also its combustion is going on.
- At $T > 300$°C, the second peak of carbon dioxide and that of H_2O coincide. This shows that the combustion process is the main process taking place.

The chemigrams of the TG/FTIR measurements under nitrogen (Fig. 6a–c) put into evidence the following points.

- As in the case of the measurements performed under air, the gas evolution begins at temperatures just above the RA melting point.
- The chemigram of CO_2 evolution shows only one peak, which does not have any appreciable counterpart in the chemigram of water evolution. Shortly after the CO_2 signal has started to increase, the signal of hydrocarbon groups also begins to increase. The decomposition pattern is similar to that obtained under air even if the hydrocarbon signal shows, under nitrogen, a sensibly higher intensity than it does in air. Moreover, the infrared spectra of the TG/FTIR experiment performed at 20°C/min show two peaks located at 3600 cm^{-1} (stretching of hydroxyl monomer) and at 1750 cm^{-1} (stretching of carbonyl of monomeric acid). Therefore, provided a fast enough heating rate is used, the evaporation of the decarboxylated residue takes place with also some direct RA evaporation.
- After the maximum hydrocarbon signal has been reached, both CO_2 and H_2O signals begin to increase. Such an increase continues up to the end of the run and it is likely to correspond to a combustion process. However, the hydrocarbon signal, although decreasing, still shows in this part of the run an higher intensity than it does in air. Thus, the last part of the measurement is a combination of evaporation and of combustion of the decarboxylated residue. As a matter of fact, at the end of the measurements, no residue is left in nitrogen (where evaporation prevails), while in air a combustion residue remains (about 20% of the initial mass).

3.2. Spectroscopic measurements

Since it has been shown that the endothermic DSC peak disappears by annealing the sample at 130°C, samples of RA have been thermally treated in oven at 130°C for different times (both under N_2 and air). These samples have been examined by various spectroscopic techniques to individuate the changes, with respect to the commercial RA sample, brought about by the thermal treatment.

3.2.1. X-Ray diffraction measurements

Fig. 7 reports the X-ray diffraction (XRD) spectra of the samples annealed at 130°C under N_2 (Fig. 7b) and under air (Fig. 7c). The spectrum of starting RA is reported (Fig. 7a), which shows only the peaks of the monoclinic phase (JCPDS file number 41-1689). The XRD spectra of the samples heated either under air or N_2 do not show any appreciable difference with respect to the monoclinic pattern for annealing temperatures up to 125°C. Seven new peaks are showing up in the sample annealed under N_2 at 130°C, all the peaks of the monoclinic RA still being present in the spectrum. Therefore, the N_2 annealed sample seems to be a mixture of two different phases: the monoclinic one, and a newly formed phase whose XRD peaks are, however, different from those of the triclinic phase (JCPDS file number 41-1690). A DSC run on the N_2-annealed sample did not show the ≈ 150°C endothermic peak, so a link can be established between the DSC peak and the formation of a new phase of RA that is different from the triclinic one. The spectrum of the sample annealed under air is quite different in that nearly

all the monoclinic phase peaks have disappeared, those of the new phase formed by nitrogen annealing are less intense or even absent, and just few new peaks are present. A DSC run also performed on this sample, does not show the endothermic peak at 150°C. It might be thought that the annealing in air leads to a partial degradation as has been brought into evidence by TGA measurements below the melting point.

A RA sample was annealed at 130°C for 66 h under N_2 flow. The XRD spectrum of this sample is reported in Fig. 7d. It can be easily seen that the spectrum resembles that of the sample annealed for 3 h at 130°C under air, with the peak intensities here being somewhat larger. Therefore, the RA thermal treatment at 130°C, besides leading to disappearance of the DSC peak at 150°C, yields the same phase obtained by the annealing under air. Clearly, the rate of transformation is higher in air than in N_2.

3.2.2. UV–Vis spectroscopy and mass spectrometry

A sample annealed at 130°C under N_2 for 66 h was examined both by UV–Vis spectroscopy and mass spectrometry. Since with both techniques the sample had to be dissolved, clearly the information about possible differences at the lattice level (molecular conformations, hydrogen bonds pattern) has been lost. Fig. 8 shows the UV–Vis spectra of a methanolic solution of commercial RA (Fig. 8a) and of the sample treated for 66 h at 130°C in N_2 (Fig. 8b). It is clearly seen that the two spectra are practically coincident. No differences between the two samples are present as concerns their molecular structure. The same information is obtained from the mass spectra of methanolic solutions of both commercial (Fig. 9a,b) and thermally treated (66 h at 130°C under N_2) samples (Fig. 10a,b) that show indistinguishable fragmentation patterns. Both the UV–Vis and mass spectrometry (MS) measurements allow one to conclude that no significant chemical differences arise from a thermal treatment that has produced a different XRD spectrum and caused the disappearance of the DSC peak at 150°C.

3.2.3. Diffuse reflectance FTIR spectroscopy

Fig. 11a,b report the diffuse reflectance FTIR spectra, respectively, of a RA commercial sample and of a thermally treated sample (66 h at 130°C under N_2). As the differences are present in the fingerprint region, only such a region is presented in the figures. These differences can be summarised as follows.

- The commercial sample shows a broad band with several maxima between 1450 and 1350 cm^{-1}, and the thermally treated one shows a broad peak at 1442 cm^{-1} that is clearly separated by a sharp peak at 1347 cm^{-1}. The hydroxyl in-plane bending vibration, coupled with the C–O stretching, is expected for the carboxylic group at 1415 ± 25 cm^{-1}. The assignment is doubtful since, in this spectral region also, the symmetric and asymmetric deformation modes of methyl groups are falling. In particular, the peak at 1347 cm^{-1} is likely to represent the symmetric bending of the $=C–CH_3$ methyl group (1380 ± 25 cm^{-1}). It could be that the thermal treatment has caused a different orientation of the side chain. If this is the case, the vibrations of C=O, O–H and C=C functional groups could also be affected.
- An α–β unsaturated carboxylic acid should show the stretching vibration of the carbonyl group at 1715–1680 cm^{-1}. In the case of commercial RA the peak is at 1684 cm^{-1}, while the thermally treated RA shows the peak at 1688 cm^{-1}. Such a slight shift towards higher frequency may result from a decrease of the H-bond strength. A difference is present also in the in-plane deformation of the carbonyl group: the commercial RA shows a peak at 696 cm^{-1} (with a doublet at ~ 730 cm^{-1}), while the thermally treated one shows the peak at 711 cm^{-1} (no doublet is present).
- The stretching of C=C conjugated with carbonyl should fall between 1680 and 1580 cm^{-1} (strong intensity). The spectrum of the commercial sample shows a peak at 1602 cm^{-1} and a double peak at 1569 and 1559 cm^{-1} (the double peak is very intense). The thermally treated sample shows only two peaks (1603 and 1572 cm^{-1}).

- The deformations of methyl and methylene groups are embedded in the broad band between 1460 and 1350 cm^{-1} in the case of the commercial RA. The different chain orientation in the thermally treated RA is also revealed by the mentioned splitting of the broad band resulting in the peaks at 1442 and 1347 cm^{-1}.
- The deformation of CH=CH (vinylene) trans group is found at 962 cm^{-1} (commercial RA) and at 969–954 cm^{-1} (doublet, thermally treated RA).
- Finally, the change in the orientation of the side chain due to the thermal treatment also affects the C=C (cyclohexene) stretching. The relevant peak falls at 1645 cm^{-1} in the commercial RA, while such a vibration does not seem to be active in the thermally treated sample.

In summary, the FTIR measurements show that, although no evidence of a real chemical modification of RA following the thermal treatment is obtained, a different orientation of the side chain has taken place that causes some vibrational changes in the fingerprint region.

4. Conclusion

The DSC peak at about 150°C corresponds to a solid-state transformation of RA. This peak no longer shows up by prolonged annealing at temperatures as low as 125–130°C. The UV–Vis and MS measurements (both in solution) do not show any difference in the molecular structure of the annealed samples. The solid-state IR spectra show evidence, mainly in the fingerprint region, of a different orientation of the side chain in thermally treated RA. The XRD patterns of the annealed samples are different from those characteristic of the monoclinic phase. They are also different from those of the triclinic phase that, as a matter of fact, we never observed. These findings point out that the thermal effect observed at 150°C has not to be attributed, as suggested by Tan et al. (1992), to the monoclinic–triclinic transition. Another RA solid phase, different from the triclinic one, is likely to be involved in that transition. Further research will be devoted to obtaining a single crystal sample of such a phase to try and refine its crystal structure.

TGA measurements show that the annealing of RA at increasing temperatures (up to 170°C, i.e. below the melting point) under nitrogen causes sublimation, while under air an oxidative degradation process occurs.

RA does not undergo a stable melting. The apparent melting enthalpy is affected by the type of sample pan used (open or closed), i.e. it depends on the exchange possibilities with the surrounding atmosphere. The decomposition under melting implies decarboxylation followed by a combined evaporation/combustion of the decarboxylated residue. The relative share of these two processes depends on the atmosphere, the combustion being the major one in air. At high heating rate (20°C/min) and in N_2, even some direct RA evaporation takes place.

References

Alam, M., Zhestkov, V., Sani, B.P., Venepally, P., Levin, A.A., Kazmer, S., Li, E., Norris, A.W., Zhang, X., Lee, M., Hill, D.L., Lin, T., Brouillette, W.J., Muccio, D.D., 1995. Conformationally defined 6-s-*trans*-retinoic acid analogs. 2. Selective agonists for nuclear receptor binding and transcriptional activity. J. Med. Chem. 38, 2302–2310.

Levin, A.H., Bos, M.E., Zusi, F.C., Nair, X., Whiting, G., Bouquin, P., Tetrault, G., Carrol, F.I., 1994. Evaluation of retinoids as therapeutic agents in dermatology. Pharm. Res. 11, 192–200.

Marini, A., Berbenni, V., Capsoni, D., Riccardi, R., Zerlia, T., 1994. Factors affecting the spectral response in a TG/FT-IR experiment. Appl. Spectrosc. 48, 1468–1471.

Muccio, D.D., Brouillette, W.J., Alam, M., Vaezi, M.F., Sani, B.P., Venepally, P., Reddy, L., Li, E., Norris, A.W., Simpson-Herren, L., Hill, D.L., 1996. Conformationally defined 6-s-*trans*-retinoic acid analogs. 3. Structure–activity relationships for nuclear receptor binding, transcriptional activity, and cancer chemopreventive activity. J. Med. Chem. 39, 3625–3635.

Muccio, D.D., Brouillette, W.J., Breritman, T.R., Taimi, M., Emanuel, P.D., Zhang, X., Chen, G., Sani, B.P., Venepally, P., Reddy, L., Alam, M., Simpson-Herren, L., Hill, D.L., 1998. Conformationally defined retinoic acid analogues. 4. Potential new agents for acute promyelocytic and juvenile myelomonocytic leukemias. J. Med. Chem. 41, 1679–1687.

Stam, C.H., McGillavry, C.H., 1963. The crystal structure of the triclinic modification of vitamin-A acid. Acta Crystallogr. 16, 62–68.

Stam, C.H., 1972. The crystal structure of a monoclinic modification and the refinement of a triclinic modification of vitamin A acid (retinoic acid), $C_{20}H_{28}O_2$. Acta Crystallogr. B28, 2936–2945.

Tan, X., Metzer, N., Lindenbaum, S., 1992. Solid-state stability studies of 13-*cis*-retinoic acid and all-trans retinoic acid using microcalorimetry and HPLC analysis. Pharm. Res. 9, 1203–1208.

Thunemann, A., Beyermann, J., von Ferber, C., Lowen, H., 2000. Immobilization of retinoic acid by polyamino acids: lamellar-structured nanoparticles. Langmuir 16, 850–857.

Thunemann, A., 1997. Immobilization of retinoic acid by cationic polyelectrolytes. Langmuir 13, 6040–6046.

Vaezi, M.F., Alam, M., Sani, B.P., Rogers, T.S., Simpson-Herren, L., Wille, J.J., Hill, D.L., Doran, T.I., Brouillette, W.J., Muccio, D.D., 1994. A conformationally defined 6-s-*trans*-retinoic acid isomer: synthesis, chemopreventive activity, and toxicity. J. Med. Chem. 37, 4499–4507.